Letter

Extreme wave excitation from localized phase-shift perturbations

Y. He [1,*] A. Witt [2,†] S. Trillo [3] A. Chabchoub [4,5,1] and N. Hoffmann [2,6,‡]

[1] *Centre for Wind, Waves and Water, School of Civil Engineering, The University of Sydney, Sydney NSW 2006, Australia*
[2] *Dynamics Group, Hamburg University of Technology, Hamburg, Germany*
[3] *Department of Engineering, University of Ferrara, via Saragat 1, 44122 Ferrara, Italy*
[4] *Hakubi Center for Advanced Research, Kyoto University, Yoshida-Honmachi, Kyoto 606-8501, Japan*
[5] *Disaster Prevention Research Institute, Kyoto University, Kyoto 611-0011, Japan*
[6] *Department of Mechanical Engineering, Imperial College London, London, United Kingdom*

(Received 17 June 2022; accepted 14 September 2022; published 21 October 2022)

The modulation instability is a focusing mechanism responsible for the formation of strong wave localizations not only on the water surface, but also in a variety of nonlinear dispersive media. Such dynamics is initiated from the injection of sidebands, which translate into an amplitude modulation of the wave field. The nonlinear stage of unstable wave evolution can be described by exact solutions of the nonlinear Schrödinger equation (NLSE). In that case, the amplitude modulation of such coherent extreme wave structures is connected to a particular phase-shift seed in the carrier wave. In this Letter, we show that phase-shift localization applied to the background, excluding any amplitude modulation excitation, can indeed trigger extreme events. Such rogue waves can be for instance generated by considering the parametrization of fundamental breathers, and thus by seeding only the local phase-shift information to the regular carrier wave. Our wave tank experiments show an excellent agreement with the expected NLSE hydrodynamics and confirm that even though delayed in their evolution, breather-type extreme waves can be generated from a purely regular wave train. Such a focusing mechanism awaits experimental confirmation in other nonlinear media, such optics, plasma, and Bose-Einstein condensates.

DOI: 10.1103/PhysRevE.106.L043101

The formation of extreme wave events, so-called rogue waves, can be understood and modeled by the nonlinear Schrödinger equation (NLSE) or its higher-order forms [1–4]. One way to control such rogue waves in a laboratory environment is by the use of fundamental breather solutions in the form of time-periodic, doubly localized, and space-periodic forms. These are also known as the Akhmediev breather (AB) [5], Peregrine breather (PB) [6], and Kuznetsov breather (KB) (also referred to in the literature as the Kuznetsov-Ma breather) [7–10], respectively. Such solutions are based on long-wave perturbation of a regular wave train with a precise dedicated phase-shift of the carrier at a specific location and instant. Even though being exact solutions of a universal weakly nonlinear wave model, breather waves are crucial in understanding the formation of extreme events in different dispersive wave systems governed by nonlinearity [11–17]. While modulation instability (MI) is usually seen as a mechanism that leads, through the amplification of sidebands, to a strong *amplitude modulation*, these phase-shifts always accompany such MI-induced amplitude reshaping. Indeed, the initial temporal phase profile, or equivalently, the input phase relationship in Fourier space (i.e., the relative phase between the MI sidebands and the central carrier), have a deep impact on the type of amplitude modulation that develops upon propagation [18,19], as recently observed experimentally [20–22].

A previous experimental study has revealed that locally the same type of maximal breather compression can be achieved by just starting from the solution's amplitude modulation of the carrier wave only and ignoring any local phase-shift in the wave field for the determination of the experiments' boundary conditions [23]. The aim of this Letter is to show that the initial phase-shift profile contains the leading information that allows the breathers to undergo the peak growth and focusing process even when the input amplitude modulation is suppressed. Indeed, our experimental investigation provides evidence that extreme wave events can be solely triggered by a localized phase-shift perturbation (PSP) of a breather solution while ignoring the amplitude modulation information. Thus, the boundary condition consists of a regular wave train with a localized PSP as determined by a fundamental breather wave envelope. Our wave maker's motion can be controlled in such a manner to locally adjust its motion to accurately generate such initial and small perturbations in a regular carrier.

To achieve this, we use specific phase-shifts proper to the three fundamental breathers, as mentioned above, and show that the extreme localization achieved in the wave flume resembles those of pure breathers, even though being spatially delayed with respect to the exact solution. In fact, the smaller the phase-shift applied to the carrier, the better is the agreement with the respective pure breather solution. All observations are in reasonable agreement with the NLSE prediction despite the very strong wave focusing reached. Our

[*] yuchen.he@sydney.edu.au
[†] andy.witt@tuhh.de
[‡] norbert.hoffmann@tuhh.de

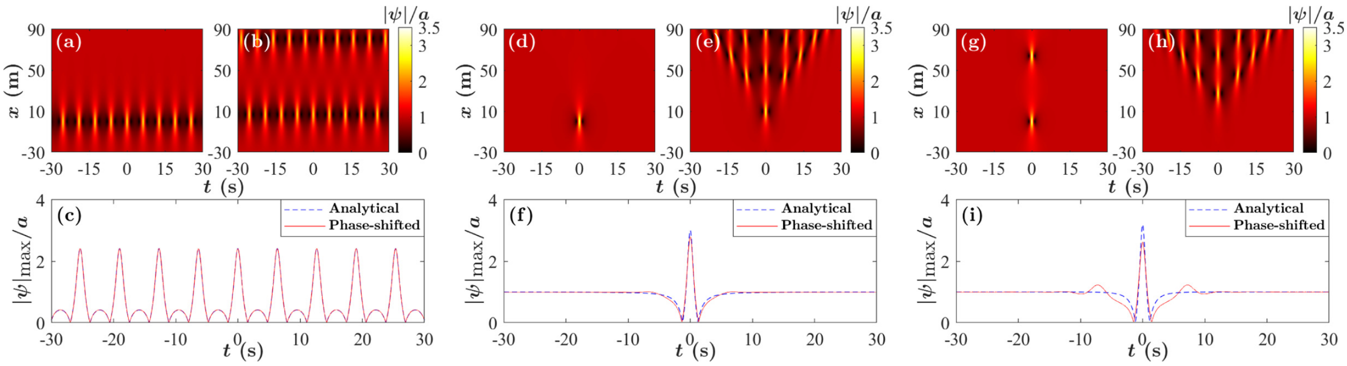

FIG. 1. (a)–(c) Akhmediev breather, contrasting spatiotemporal evolutions arising from (a) the full analytical solution and (b) the phase-shift perturbation (PSP); (c) temporal profile of the exact solution compared to that generated from the PSP at the location of maximal compression. (d)–(f) Peregrine breather, contrasting spatiotemporal evolutions arising from (d) the full solution and (e) the PSP; (f) comparison of transverse profiles at maximal compression. (g)–(i) Kuznetsov breather, contrasting spatiotemporal evolutions arising from (g) the full solution and (h) the PSP; (i) comparison of transverse profiles at maximal compression. Here, the adopted carrier wave steepness $ak = 0.1$ and carrier amplitude $a = 0.01$ m. All waves are excited at $x^* = -30$ m, i.e., 30 m ahead of the first focus point ($x^* = 0$) of the exact solution.

results suggest that the analysis of ocean rogue waves should also comprise the local phase information to fully understand the early stage of formation.

The NLSE is the simplest framework to describe the wave propagation of nonlinear dispersive waves [24]. For the deep-water wave problem, the slowly varying wave envelope $\Psi(x,t)$ around the wave number k satisfies [2,25]

$$i\left(\frac{\partial \Psi}{\partial x} + \frac{2k}{\omega}\frac{\partial \Psi}{\partial t}\right) - \frac{k}{\omega^2}\frac{\partial^2 \Psi}{\partial t^2} - k^3|\Psi|^2\Psi = 0, \tag{1}$$

where $\omega = \sqrt{gk}$ is the dispersion relation, g being the gravitational acceleration.

As a result of integrability a variety of steady and pulsating solutions have been derived [26,27]. We will not recall the parametrization of three fundamental breathers on a finite-amplitude carrier as these have been discussed in many past publications [10,28–30]. The family of ABs describe the nonlinear stage of MI and are periodic in time when considering the framework (1), the PB is the limit case of zero modulation frequency, i.e., infinite modulation period, and the KBs the space periodic solution, which starts its evolution from a solitonic perturbation on the carrier. As such, the KB never converges to a uniform amplitude. All these solutions have been observed in a variety of nonlinear dispersive media and, for more details, we refer the reader to Refs. [10,28–31]. In water waves the boundary conditions at beginning of the flume consist of a time series of surface displacements. The latter are driving the wave maker while its mechanical motion is linearly proportional to the surface elevation signal as determined by theory. To drive the wave maker and to observe NLSE solitons or breathers, it is sufficient to use the expression of surface elevation defined to first order of approximation [31]

$$\eta(x,t) = \mathrm{Re}\{\Psi(x,t)\exp\left[i(kx - \omega t)\right]\}. \tag{2}$$

Given an amplitude of the background a, the hydrodynamic deep-water Akhmediev, Peregrine, or Kuznetsov breather $\Psi(x,t)$ can be parametrized as follows [10,20,32]:

$$\Psi_{\mathrm{AB/KB/PB}}(x,t) = a\left(1 + \frac{2(1-2\mathfrak{a})\cosh\left(a^2k^3\mathfrak{b}x\right) - i\mathfrak{b}\sinh\left(a^2k^3\mathfrak{b}x\right)}{\sqrt{2\mathfrak{a}}\cos\left[\frac{ak\omega}{\sqrt{2}}\Omega\left(t - \frac{x}{c_g}\right)\right] - \cosh\left(a^2k^3\mathfrak{b}x\right)}\right) \times \exp(-ia^2k^3x), \tag{3}$$

$\mathfrak{b} = \sqrt{8\mathfrak{a}(1-2\mathfrak{a})}$, and $\Omega = 2\sqrt{1-2\mathfrak{a}}$. For $0 < \mathfrak{a} < 0.5$, $\Psi(x,t)$ is the Akhmediev breather (maximal growth rate when $\mathfrak{a} = 0.25$), while for $\mathfrak{a} > 0.5$, $\Psi(x,t)$ is the Kuznetsov breather. When $\mathfrak{a} \longrightarrow 0.5$, $\Psi(x,t)$ converges to the rational Peregrine breather solution [6,29].

As mentioned in Ref. [23], each of these exact solutions $\Psi(x,t)$ can be written as the amplitude modulation function $A(x,t)$ and a respective phase-shift $\phi(x,t)$, both evolving in time and space. Mathematically speaking, $\Psi(x,t) = A(x,t)\exp[i\phi(x,t)]$. Also in the latter work, it has been shown that wave-breather-like focusing can develop when starting from boundary conditions at beginning of the flume, involving the amplitude modulation only without consideration of the breather-specific local phase-shift.

Next, we propose an extreme wave focusing mechanism, which originates in a regular and amplitude-modulation-free wave train, with a PSP, i.e., a localized phase-shift. While a similar mechanism was originally investigated theoretically in Ref. [33] for abrupt phase jumps, in this Letter, we rather consider the PSP obtained by impressing the localized phase profile of the pure breather solution at a given distance from the focus point. Examples of evolution, obtained from the NLSE (1) are shown in Figs. 1(a)–1(c) for the AB, in Figs. 1(d)–1(f) for the PB, and in Figs. 1(g)–1(i) for the KB. In all examples $x^* = 0$ stands for the first focus point, and the PSP is excited at $x^* = -30$ m. As shown, in all three different breather cases considered, a strong wave envelope compression is expected to occur in the condensate from a PSP triggering only. We emphasize that the smaller the

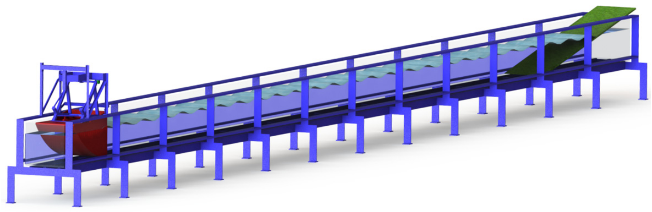

FIG. 2. The University of Sydney's 30 m water wave tank comprising a piston-type wave maker and an artificial-grass wave absorbing beach installation.

amplitude modulation as defined by the exact solution, and as such the smaller the phase-shift, the better the agreement of maximal envelope compression profiles between the NLSE solution and the one resulting from the PSP-initialization. Note that similarly to the mechanism studied in Ref. [23], the location of maxima deviates and is retarded compared to the motion of the exact solution. Moreover, we can clearly notice that deviations are rather substantial when considering the KB case. The reason for this is that the solution never converges to the background and thus triggering the boundary conditions from a regular wave train with $\phi_{\mathrm{KB}}(x^*, t)$ will substantially deviate compared to the AB- or PB-type dynamics. In any event, the PSP-induced dynamics for both the PB and the KB cases show a postfocusing dynamics dominated by fissions into pairs of quasi-KB breathers with opposite velocities [23], whose observation, however, requires wave facility with a length far exceeding that of the present installation.

In the following we report on our experimental investigation. We adopt the same setup as described in Ref. [16] and depicted in Fig. 2.

The wave facility has a length of 30 m with an effective wave propagation distance of 25 m when considering the wave absorbing installation opposite to the piston-type wave maker. The water depth adopted is of $h = 0.7$ m and the carrier wave number is chosen to satisfy operations in the deep-water regime, i.e., $kh > \pi$. In fact, the carrier parameters will be defined by the wave steepness parameter ak and carrier amplitude a. The wave number k and wave frequency ω are connected through the linear dispersion relation as mentioned above. The wave gauges' temporal resolution is 0.03 s while the spatial resolution is 0.3 m. To extract the wave envelope dynamics in time and space, we first apply the Hilbert transform to each collected and bandpass-filtered surface elevation time series. A bandpass filter is crucial to exclude the effects of bound waves and subsequent oscillation of the wave envelope [2,34]. As a next step, we interpolate and apply a moving-average smoothing. Moreover, we emphasize that injected phase-shift $\phi(x^*, t)$, as defined by the breather solution, is chosen to be small to enable the proper generation of a regular wave train by the wave maker. In fact, because the linear wave maker's transfer function is frequency dependent, initiating the experiments from a large PSP could compromise the steadiness of wave amplitude generation. As such, the PSP must be small, i.e., as defined at a location of early stage of breather initialization and focusing. Indeed, the smaller the carrier perturbation of an AB or PB, i.e., the smaller x^*, the smaller is the phase-shift [35,36]. The choice of x^* is bound

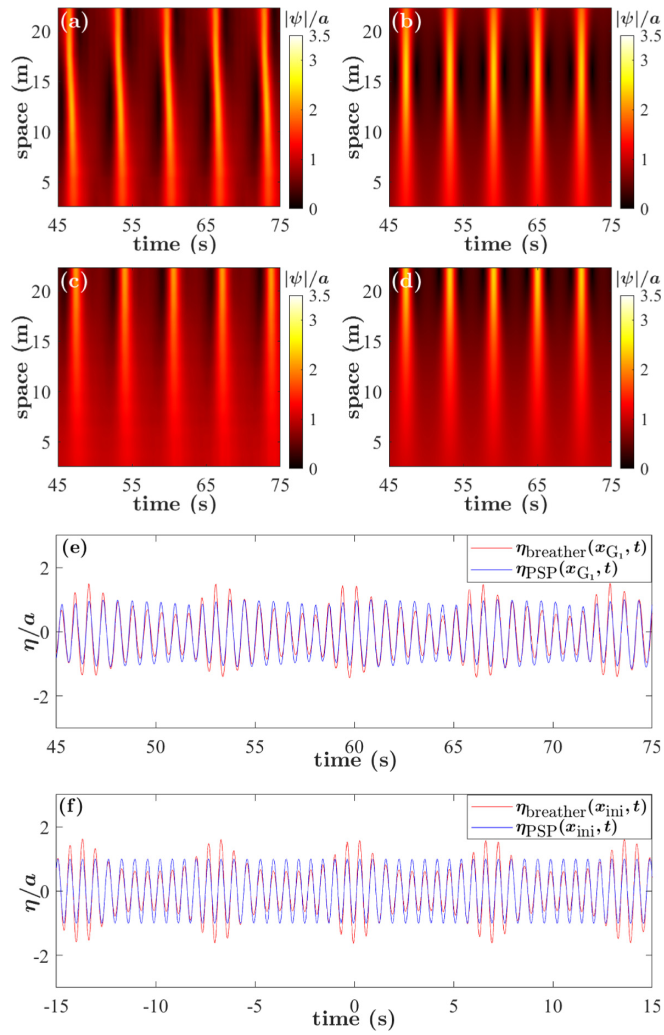

FIG. 3. AB evolution for $ak = 0.12$ and $a = 0.01$ m with an expected amplitude amplification of 2.41 (the case of maximal growth rate). (a) Propagation of the wave envelope as measured in the flume. (b) NLSE simulations with the same boundary conditions as in (a). (c) Experimental observation of the AB-PSP in the regular background case. (d) NLSE simulations with the same boundary conditions as in (c). (e) Analytical and phase-shifted AB wave elevation at 2.5 m from the wave maker, which corresponds to the location of the first gauge G_1. (f) Analytical and phase-shifted AB wave elevation boundary conditions at $x^* = -16$ m as implemented in the experiments and simulations.

by the length of the wave facility to allow for the observation of the complete first focusing within the tank length for either the exact breather or the respective case of breather PSP in the regular carrier wave. This also applies to the carrier wave parameters, which must be cautiously chosen too. Note that the imposed phase-shift is still larger than any experimental noise.

As a starting point, our experimental investigation is initiated by investigating the AB dynamics triggered by both exact and PSP configurations as discussed above and illustrated in Figs. 1(a)–1(c). The results are shown in Fig. 3.

All collected measurements of the exact time-periodic breather show a reasonable agreement with NLSE theory.

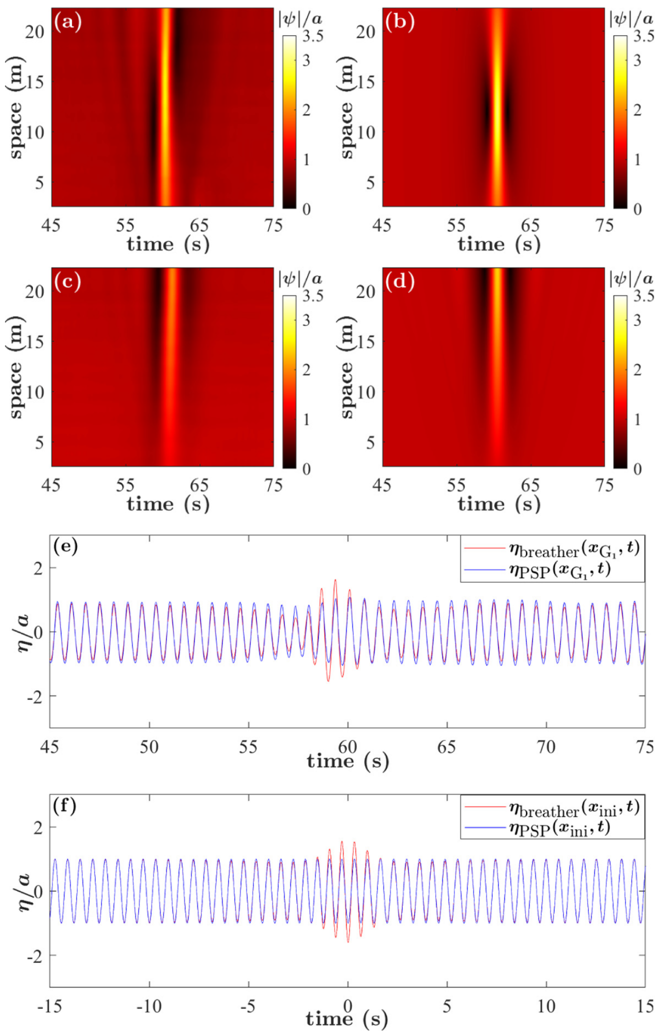

FIG. 4. PB evolution for $ak = 0.1$ and $a = 0.01$ m with an expected theoretical amplitude amplification of 3. (a) Propagation of the wave envelope as measured in the flume. (b) NLSE simulations with the same boundary conditions as in (a). (c) Experimental observation of the PB-PSP in the regular background case. (d) NLSE simulations with the same boundary conditions as in (c). (e) Analytical and phase-shifted PB wave elevation at 2.5 m from the the wave maker, which corresponds to the location of the first gauge G_1. (f) Analytical and phase-shifted PB wave elevation boundary conditions at $x^* = -12$ m as implemented in the experiments and simulations.

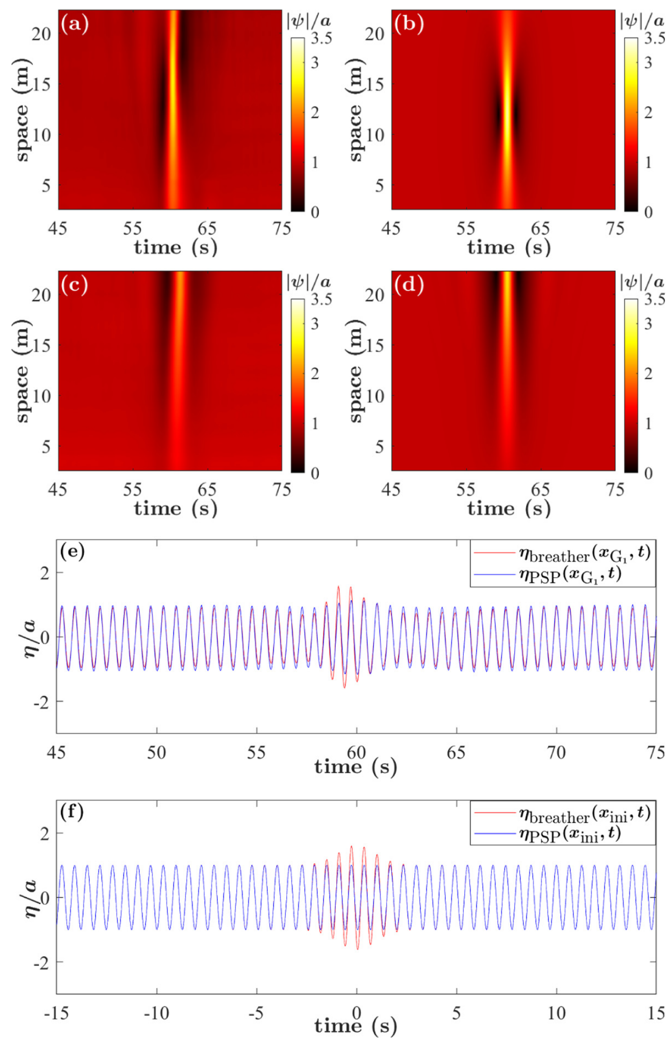

FIG. 5. KB evolution for $ak = 0.1$ and $a = 0.01$ m with an expected amplitude amplification of 3.3. (a) Propagation of the wave envelope as measured in the flume. (b) NLSE simulations with the same boundary conditions as in (a). (c) Experimental observation of the KB-PSP in the regular background case. (d) NLSE simulations with the same boundary conditions as in (c). (e) Analytical and phase-shifted KB wave elevation at 2.5 m from the wave maker, which corresponds to the location of the first gauge G_1. (f) Analytical and phase-shifted KB wave elevation boundary conditions at $x^* = -12$ m as implemented in the experiments and simulations.

This applies for both the case when considering the pure AB solution of the NLSE and the regular wave train in which the AB-type phase-shift has been locally seeded. Remarkably, a gradual focusing clearly emerges from the phase-shift seeding, in agreement with the numerical NLSE expectations.

The same excellent agreement in the wave focusing is also observed for case of PB, which is illustrated in Fig. 4.

In this case one particular feature of focusing from the PSP in the background of constant amplitude becomes clear. The retardation and delay in the focusing from the single unstable Peregrine packet is noticeable. A similar feature has been observed when ignoring the breather-specific phase-shift and considering only the amplitude modulation [23]. These observations also expose the limitations of our experimental setup. Since we start from a small phase-shift value in the carrier, the retardation of maximal wave focusing of the waves would require a long fetch to observe interesting postfocusing dynamics (recurrence, triangular patterns, etc.). This is also the case for the KB. We chose the case of an amplitude focusing factor of 3.3 and as the previous breather cases, the two types of wave envelope dynamics are shown in Fig. 5.

We annotate that we employ the same color-bar scale in all the figures to make significant wave focusing more distinct. Overall, all cases show a reasonable good agreement with the weakly nonlinear NLSE framework approximated from the Euler equations to third order in steepness. That said, a typical wave asymmetry is clearly noticeable in the experimental data. The latter can be explained and modeled by the modified

NLSE accounting for fourth-order effects in steepness in the form of higher-order dispersion and mean flow [37–39]. These effects captured by the modified NLSE [40] were also observed and studied in more recent experiments in the context of nonlinear wave-packet evolution [17,41,42].

In summary, we have reported an experimental study confirming a proof of concept that rogue waves can appear from a localized PSP in a regular wave train. Such PSP can be for instance constructed from breather solutions of the nonlinear Schrödinger equation, and then seeded in a condensate. Our wave tank measurements underline that nonlinear focusing can be exhibited by PSP, confirming yet another focusing mechanism beyond the wave modulation or superposition principle. We anticipate future experimental studies exploring such focusing dynamics in various wave systems governed by dispersion and nonlinearity [11,43,44] and also the development of theoretical techniques to predict such dynamics within the NLSE framework and beyond [45,46].

[1] N. N. Akhmediev and A. Ankiewicz, *Solitons: Nonlinear Pulses and Beams* (Chapman & Hall, London, 1997).

[2] A. Osborne, *Nonlinear Ocean Waves and the Inverse Scattering Transform* (Academic Press, Cambridge, MA, 2010).

[3] M. Onorato, S. Residori, U. Bortolozzo, A. Montina, and F. Arecchi, Rogue waves and their generating mechanisms in different physical contexts, Phys. Rep. **528**, 47 (2013).

[4] J. M. Dudley, F. Dias, M. Erkintalo, and G. Genty, Instabilities, breathers and rogue waves in optics, Nat. Photon. **8**, 755 (2014).

[5] N. Akhmediev, V. Eleonskii, and N. Kulagin, Generation of periodic trains of picosecond pulses in an optical fiber: exact solutions, Sov. Phys. JETP **62**, 894 (1985).

[6] D. H. Peregrine, Water waves, nonlinear Schrödinger equations and their solutions, J. Aust. Math. Soc. Ser. B **25**, 16 (1983).

[7] E. A. Kuznetsov, Solitons in a parametrically unstable plasma, Dokl. Akad. Nauk SSSR **236**, 575 (1977).

[8] Y.-C. Ma, The perturbed plane-wave solutions of the cubic Schrödinger equation, Stud. Appl. Math. **60**, 43 (1979).

[9] K. B. Dysthe and K. Trulsen, Note on breather type solutions of the NLS as models for freak-waves, Phys. Scr. **T82**, 48 (1999).

[10] B. Kibler, J. Fatome, C. Finot, G. Millot, G. Genty, B. Wetzel, N. Akhmediev, F. Dias, and J. M. Dudley, Observation of Kuznetsov-Ma soliton dynamics in optical fibre, Sci. Rep. **2**, 463 (2012).

[11] B. Frisquet, B. Kibler, and G. Millot, Collision of Akhmediev Breathers in Nonlinear Fiber Optics, Phys. Rev. X **3**, 041032 (2013).

[12] N. Vishnu Priya, M. Senthilvelan, and M. Lakshmanan, Akhmediev breathers, Ma solitons, and general breathers from rogue waves: A case study in the Manakov system, Phys. Rev. E **88**, 022918 (2013).

[13] H. Xiong and Y. Wu, Optomechanical Akhmediev breathers, Laser Photon. Rev. **12**, 1700305 (2018).

[14] E. C. Aslan and M. Inc, Optical soliton solutions of the NLSE with quadratic-cubic-Hamiltonian perturbations and modulation instability analysis, Optik **196**, 162661 (2019).

[15] A. Houwe, M. İnç, S. Doka, M. Akinlar, and D. Baleanu, Chirped solitons in negative index materials generated by Kerr nonlinearity, Results Phys. **17**, 103097 (2020).

[16] Y. He, A. Slunyaev, N. Mori, and A. Chabchoub, Experimental Evidence of Nonlinear Focusing in Standing Water Waves, Phys. Rev. Lett. **129**, 144502 (2022).

[17] G. G. Rozenman, W. P. Schleich, L. Shemer, and A. Arie, Periodic Wave Trains in Nonlinear Media: Talbot Revivals, Akhmediev Breathers, and Asymmetry Breaking, Phys. Rev. Lett. **128**, 214101 (2022).

[18] S. Trillo and S. Wabnitz, Dynamics of the nonlinear modulational instability in optical fibers, Opt. Lett. **16**, 986 (1991).

[19] A. Armaroli, A. Gomel, A. Chabchoub, M. Brunetti, and J. Kasparian, Stabilization of uni-directional water wave trains over an uneven bottom, Nonlin. Dyn. **101**, 1131 (2020).

[20] O. Kimmoun, H. C. Hsu, H. Branger, M. S. Li, Y. Y. Chen, C. Kharif, M. Onorato, E. J. R. Kelleher, B. Kibler, N. Akhmediev, and A. Chabchoub, Modulation instability and phase-shifted Fermi-Pasta-Ulam recurrence, Sci. Rep. **6**, 28516 (2016).

[21] A. Mussot, C. Naveau, M. Conforti, A. Kudlinski, F. Copie, P. Szriftgiser, and S. Trillo, Fibre multi-wave mixing combs reveal the broken symmetry of Fermi–Pasta–Ulam recurrence, Nat. Photon. **12**, 303 (2018).

[22] D. Pierangeli, M. Flammini, L. Zhang, G. Marcucci, A. J. Agranat, P. G. Grinevich, P. M. Santini, C. Conti, and E. DelRe, Observation of Fermi-Pasta-Ulam-Tsingou Recurrence and Its Exact Dynamics, Phys. Rev. X **8**, 041017 (2018).

[23] A. Chabchoub, T. Waseda, M. Klein, S. Trillo, and M. Onorato, Phase-suppressed hydrodynamics of solitons on constant-background plane wave, Phys. Rev. Fluids **5**, 114801 (2020).

[24] M. J. Ablowitz, *Nonlinear Dispersive Waves: Asymptotic Analysis and Solitons* (Cambridge University Press, Cambridge, UK, 2011), Vol. 47.

[25] V. E. Zakharov, Stability of periodic waves of finite amplitude on the surface of a deep fluid, J. Appl. Mech. Tech. Phys. **9**, 190 (1968).

[26] V. E. Zakharov and A. B. Shabat, Exact theory of two-dimensional self-focusing and one-dimensional self-modulation of waves in nonlinear media, Sov. Phys. JETP **34**, 62 (1972).

[27] N. Akhmediev, Waves that appear from nowhere: Complex rogue wave structures and their elementary particles, Front. Phys. **8**, 612318 (2021).

[28] J. M. Dudley, G. Genty, F. Dias, B. Kibler, and N. Akhmediev, Modulation instability, Akhmediev breathers, and rogue waves in nonlinear fiber optics, in *Fiber Lasers VII: Technology, Systems, and Applications* (SPIE, 2010), Vol. 7580, pp. 615–620.

[29] B. Kibler, J. Fatome, C. Finot, G. Millot, F. Dias, G. Genty, N. Akhmediev, and J. M. Dudley, The Peregrine soliton in nonlinear fibre optics, Nat. Phys. **6**, 790 (2010).

[30] A. Chabchoub and R. H. Grimshaw, The hydrodynamic nonlinear Schrödinger equation: Space and time, Fluids **1**, 23 (2016).

[31] A. Chabchoub, N. P. Hoffmann, and N. Akhmediev, Rogue Wave Observation in a Water Wave Tank, Phys. Rev. Lett. **106**, 204502 (2011).

[32] J. M. Dudley, G. Genty, F. Dias, B. Kibler, and N. Akhmediev, Modulation instability, Akhmediev breathers and continuous wave supercontinuum generation, Opt. Express **17**, 21497 (2009).

[33] A. Sheveleva and C. Finot, Temporal Fresnel diffraction induced by phase jumps in linear and nonlinear optical fibres, Results Phys. **19**, 103344 (2020).

[34] D. Eeltink, A. Armaroli, C. Luneau, H. Branger, M. Brunetti, and J. Kasparian, Separatrix crossing and symmetry breaking in NLSE-like systems due to forcing and damping, Nonlin. Dyn. **102**, 2385 (2020).

[35] G. Xu, K. Hammani, A. Chabchoub, J. M. Dudley, B. Kibler, and C. Finot, Phase evolution of Peregrine-like breathers in optics and hydrodynamics, Phys. Rev. E **99**, 012207 (2019).

[36] Y. He, P. Suret, and A. Chabchoub, Phase evolution of the time- and space-like Peregrine breather in a laboratory, Fluids **6**, 308 (2021).

[37] K. Trulsen and C. T. Stansberg, Spatial evolution of water surface waves: Numerical simulation and experiment of bichromatic waves, in *The Eleventh International Offshore and Polar Engineering Conference* (OnePetro, Richardson, TX, 2001).

[38] L. Shemer and L. Alperovich, Peregrine breather revisited, Phys. Fluids **25**, 051701 (2013).

[39] A. Slunyaev, E. Pelinovsky, A. Sergeeva, A. Chabchoub, N. Hoffmann, M. Onorato, and N. Akhmediev, Super rogue waves in simulations based on weakly nonlinear and fully nonlinear hydrodynamic equations, Phys. Rev. E **88**, 012909 (2013).

[40] K. B. Dysthe, Note on a modification to the nonlinear Schrödinger equation for application to deep water waves, Proc. R. Soc. London, Ser. A **369**, 105 (1979).

[41] G. G Rozenman, S. Fu, A. Arie, and L. Shemer, Quantum mechanical and optical analogies in surface gravity water waves, Fluids **4**, 96 (2019).

[42] G. G. Rozenman, L. Shemer, and A. Arie, Observation of accelerating solitary wavepackets, Phys. Rev. E **101**, 050201(R) (2020).

[43] I. Kourakis, M. Mc Kerr, and A. Ur-Rahman, Semiclassical relativistic fluid theory for electrostatic envelope modes in dense electron–positron–ion plasmas: Modulational instability and rogue waves, J. Plasma Phys. **79**, 1089 (2013).

[44] D. Luo, Y. Jin, J. H. V. Nguyen, B. A. Malomed, O. V. Marchukov, V. A. Yurovsky, V. Dunjko, M. Olshanii, and R. G. Hulet, Creation and Characterization of Matter-Wave Breathers, Phys. Rev. Lett. **125**, 183902 (2020).

[45] P. Suret, A. Tikan, F. Bonnefoy, F. Copie, G. Ducrozet, A. Gelash, G. Prabhudesai, G. Michel, A. Cazaubiel, E. Falcon, G. El, and S. Randoux, Nonlinear Spectral Synthesis of Soliton Gas in Deep-Water Surface Gravity Waves, Phys. Rev. Lett. **125**, 264101 (2020).

[46] R. Mullyadzhanov and A. Gelash, Solitons in a Box-Shaped Wave Field with Noise: Perturbation Theory and Statistics, Phys. Rev. Lett. **126**, 234101 (2021).